Original Article

Vascular

Vascular
2025, Vol. 33(3) 548–555

DOI: 10.1177/17085381241257161
journals.sagepub.com/home/vas
Sage

Hemodynamic analysis of thoracic endovascular aortic repair with left subclavian artery reconstructed by chimney stent

Yunpeng Ding[1], Chunbo Xu[1], Tiequan Yang[2], Shuyuan Wang[1], Di Wang[1], Songjie Hu[1] and Dehai Lang[1]

Abstract

Objectives: The purpose of this study was to investigate the hemodynamic consequences of thoracic endovascular aortic repair which reconstructed left subclavian artery by chimney stent (ch-TEVAR).

Methods: Two patients who underwent thoracic endovascular aortic repair (TEVAR) and left subclavian artery (LSA) reconstruction using chimney stents were selected. Preoperative and postoperative CTA images were collected to reconstruct hemodynamic models for comparing and analyzing blood pressure, blood flow velocity, and wall shear stress in the aortic arch and its major branches. Concurrently, morphological alterations and position of chimney stent were also assessed.

Results: After the reconstruction of LSA in ch-TEVAR, no endoleak was seen, but the stent in LSA was compressed. The blood flow velocity of the LSA increased and disordered, the pressure was reduced, and the WSS was increased. Even more, there were a large amount of turbulence found in the LSA of one case, and its LSA was blocked.

Conclusion: Chimney stent reduces the occurrence of endoleak due to its excellent deformation ability, but the compressed stent has a greater impact on the hemodynamics of LSA and eventually leads to LSA occlusion; in order to keep the LSA unobstructed, it is necessary to pay attention to the position of the chimney stent and keep it straight and do not fold or twist. Chimney stent has little influence on the aortic arch and the rest of the aortic arch branches.

Keywords

Left subclavian revascularization, hemodynamics, endoleak, computational fluid dynamics, chimney stent

Introduction

Thoracic endovascular aortic repair (TEVAR) has progressively emerged as the primary therapeutic strategy for aortic pathologies, garnering considerable attention.[1,2] Standard TEVAR necessitates a proximal anchoring zone exceeding 20 mm.[3] In a multitude of instances, addressing aortic arch lesions requires stent coverage of LSA to achieve sufficient anchoring area.[4] Nonetheless, direct LSA coverage during TEVAR may contribute to heightened incidences of complications, including stroke, spinal cord ischemia, and left upper limb ischemia.

In recent years, an escalating number of investigations have posited that LSA revascularization, as opposed to direct coverage, may yield more favorable overall prognostic outcomes.[5–7] Reconstructive methodologies encompass open surgical techniques such as bypass surgery; endovascular reconstruction includes chimney, fenestration, and custom stent techniques.[8–10] Although open surgery proves efficacious, it also exhibits a traumatic nature and a propensity for complications. Fenestration techniques or custom stents have demonstrated promising results in select studies, yet these approaches remain constrained by aortic arch morphological diversity, patient-specific factors, and custom device availability. Consequently, they are typically

[1]Department of Vascular Surgery, Ningbo No.2 Hospital, Ningbo, China
[2]Department of Interventional Radiology, Ningbo No.2 Hospital, Ningbo, China

Corresponding author:
Dehai Lang, Department of Vascular Surgery, Ningbo No.2 Hospital, No. 41 northwest Street, Ningbo, Zhejiang, 315000, China.
Email: ningbo2vascular@126.com

unsuitable for emergency circumstances. Some off-the-shelf thoracic branch stent grafts, such as Gore Thoracic Branch Endoprosthesis, which are suitable for TEVAR requiring extension of proximal seal into zone 2, unfortunately, are not widely used in some countries because of health care policies. The chimney technique, a crucial alternative for conserving aortic branches, was initially reported by Criado as a means of reconstructing the left subclavian artery.[11] This technique affords the advantage of utilizing standard off-the-shelf equipment and exhibits relative ease of operation. Its application in TEVAR has broadened in recent years.[12] However, the long-term efficacy of the chimney technique remains predominantly undetermined. Current concerns focus on the risks of endoleak associated with chimney stent and the impact of chimney stent on hemodynamics.[13–16]

Hemodynamic parameters will help evaluate the impact of chimney stents and help clinicians improve ch-TEVAR surgery. Since comprehensive hemodynamics cannot be obtained with current clinical measurement techniques, computational fluid dynamics (CFD) is widely used to capture blood flow characteristics.[17–19] In this study, two patient-specific 3D hemodynamic models were reconstructed to demonstrate the influence of chimney stent on hemodynamics.

Materials and methods

Patient selection

This study reviewed the medical records of two patients who underwent ch-TEVAR for aortic disease admitted between 2020 and 2021. Informed consent to be included in the study was obtained from each patient. Case 1 was a 46-year-old female patient, diagnosed with intramural hematoma. Case 2 was a 64-year-old female, diagnosed with aortic dissection. They all had severe chest pain that is difficult to relieve. Their aortic disease involved LSA. Their preoperative CTA is shown in Figure 1. In order to obtain adequate proximal landing zone and revascularization of LSA, they were treated with ch-TEVAR.

Endovascular Procedure

All aortic lesions were analyzed by two specialists with >10 years of preoperative evaluation experience. Super size is not greater than 10%. Finally, the stent deployment was determined based on intraoperative aortography. Percutaneous access to the left brachial artery (LBA) was obtained to deploy the 6F sheath, and a 5F angiography catheter was then inserted through the guide wire into the ascending aorta for aortography. The 11F sheath was inserted into the exposed femoral artery. The catheter was placed into the ascending aorta and then replaced with a superstiff guide wire through which the main stent enters the aortic arch. Case 1 used Hercules (MicroPort, Shanghai, China) as the main stent and Case 2 used Ankura (Lifetech, Shenzhen, China). Main stent implantation was performed when the systolic pressure was less than 90 mmhg. Through the sheath of the left brachial artery, a stiff guide wire was placed over a caudate catheter into the ascending aorta. Viabahn (W. L. Gore & Associates, Flagstaff, USA) stent implantation was used to preserve LSA. Case 1 used 9*50 mm Viabahn and Case 2 used 8*50 mm Viabahn as the chimney stent. The proximal part of the chimney stent exceeded the leading edge of the main stent, and the distal part of the chimney stent uncovered the vertebral artery. The fine tail catheter was pushed into the ascending aorta by hard guide wire. Aortography was performed immediately to confirm that the internal leakage had been excluded and the arch branch artery was patency.

Follow-up

All patients participated in postoperative follow-up every year to assess relevant symptoms and syndromes. Aortic CTA was collected 1 year after ch-TEVAR to establish 3D model. At the same time, two physicians assessed preoperative and postoperative CTA, observing the aorta for deformation, endoleak, and changes in shape and position of stent, such as folding, twisting, and displacement.

Mesh generation and CFD simulations

3D models were generated with raw DICOM data form CTA of patients and processed using Mimics 21.0 (Materialise, Belgium). The three superior aortic branches were retained, and the other descending aortic branches were excluded for simplicity. All the geometric boundaries of inlet and outlets were cropped to get a flat surface in Geomagic Studio (Geomagic Inc, USA).

Hemodynamic computations were performed on the 3D arterial model presented. The Navier–Stokes (NS) equations (Figure 2(a)) for 3D time-dependent blood flows were solved using a finite-volume-based CFD solver developed by Boea Wisdom (Hangzhou) Network Technology Co. Ltd (https://www.boea-wisdom.com). The blood was considered as Newtonian and incompressible with a density of 1060 kg/m3 and dynamic viscosity of 0.004 Pa s.[20] The vessel wall was assumed to be non-slip and rigid. The three-element Windkessel model (WK3)[21] was coupled to each outlet. WK3 parameters were calibrated[22] to match the measured systolic and diastolic pressures and the estimated fraction of CO leaving each outlet. The inlet flow rate was obtained by adjusting a typical ascending aorta blood flow waveform [23] to meet patient-specific hemodynamic data (cardiac output (CO), heart rate, and systolic to diastolic duration ratio,

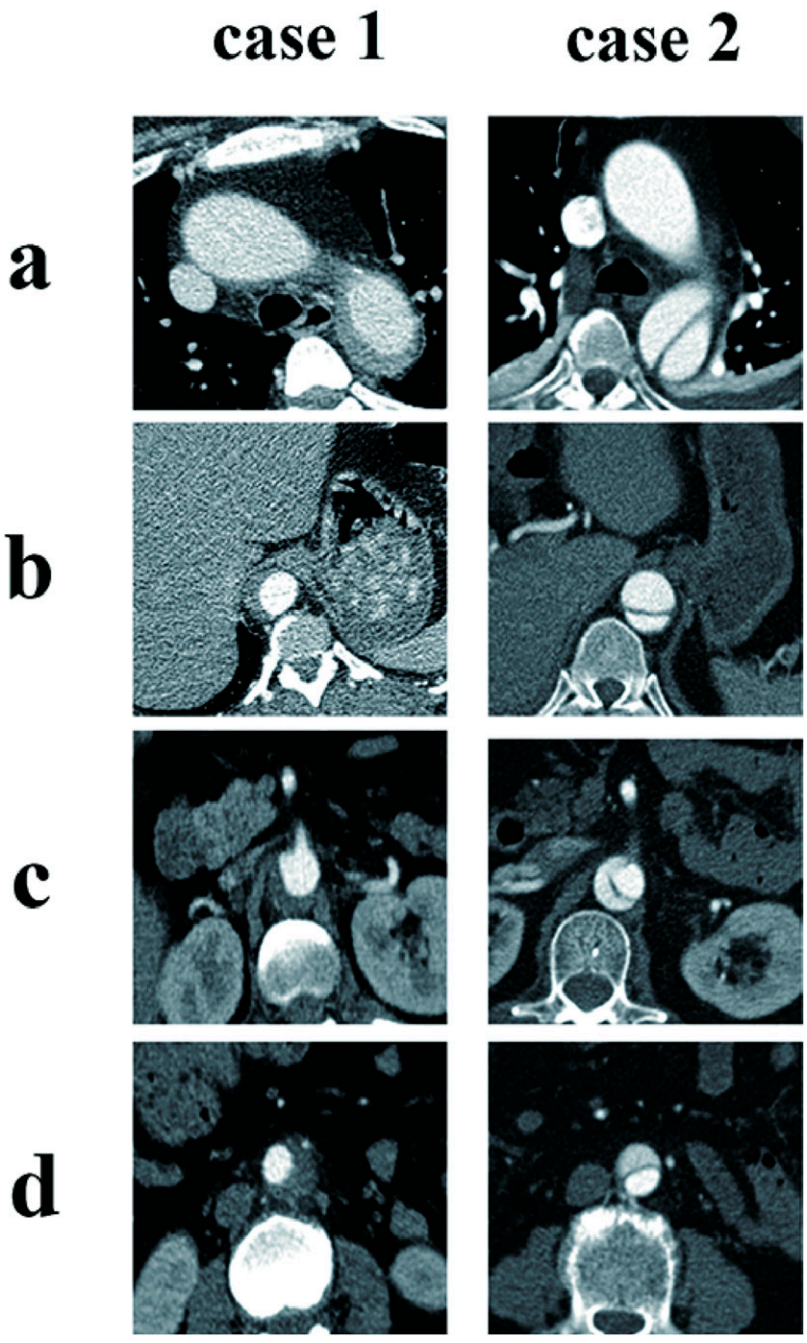

Figure 1. Preoperative CTA of Case 1 and Case 2. (a) Aortic arch area. (b) Descending aorta area. (c) Visceral area. (d) Abdominal aortic area.

Figure 2(b)). The NS equations were spatially and temporally discretized with a second-order upwind scheme and a first-order implicit Euler scheme, respectively. The 3D aortic model was discretized by tetrahedral elements with size varying from 0.1 to 0.2 mm in the fluid region. The number of elements in the generated mesh was about 7376.1 thousand elements. A constant time step of 10 ms was chosen, which was sufficient to achieve time independence. The convergence of the solution was controlled by specifying a maximum root mean square residual of 10^{-5}. The simulations were run for three cardiac cycles to reach periodic steady state, and only the systolic peak of the last cycle was retained for further analysis.

Results

Clinical outcomes

The surgical procedures for two patients were successful, with no adverse events such as bleeding, stroke, paraplegia, infection, or death during the perioperative period. Throughout the clinical follow-up, there were no reports of chest and back pain, limb weakness, and no endoleak was recorded in any patient.

Stent morphological alterations

In all cases, stents remained in their original positions as placed during surgery. Chimney stents experienced compression in the contact area with the main stents but no displacement. In Case 1, chimney stent was placed straight on one side of the main stent and Case 1's chimney stent is compressed by 25% at the extrusion point between the chimney stent and the main stent, while in Case 2, chimney stent, which was situated atop the primary chimney, and even twist, compressed by 65% and nearly occluded, as illustrated in Figure 3.

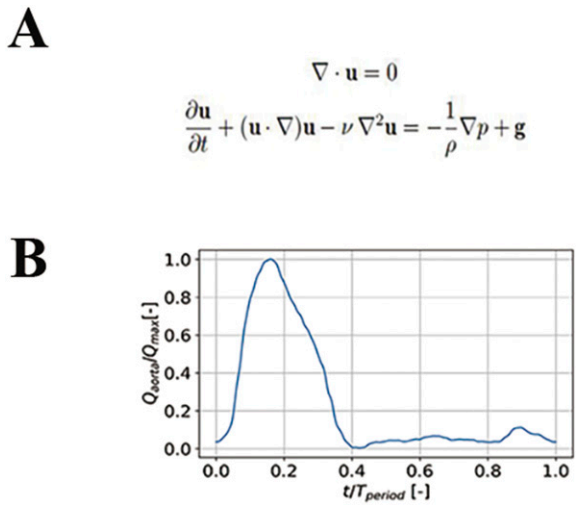

Figure 2. (a) Navier–Stokes (NS) equations. (b) Ascending aorta blood flow waveform.

Hemodynamic characteristics

Based on the analysis of hemodynamic model, no significant hemodynamic changes were found in the aortic arch, the brachiocephalic trunk, the left common carotid artery, and the visceral segment of descending aorta. The LSA in all two patients experienced varying degrees of compression, leading to hemodynamic alterations: Figure 4(a) shows the flow velocity for two cases. In Case 1 and Case 2, there was no significant difference in blood flow velocity in aortic arch, brachiocephalic trunk, left common carotid artery, and descending aorta after ch-TEVAR. However, the blood flow velocity was significantly increased and blood flow became disordered at the compression site of the chimney stent in LSA of Case 1 and Case 2 after ch-TEVAR (preoperation vs postoperation: 0.18 m/s vs 0.6 m/s in Case 1 and 0.25 m/s vs 0.7 m/s in Case 2). Moreover, in Case 2, the stent was severely compressed and close to occlusion, and there was obvious turbulence when blood flow passed.

Wall shear stress (WSS) is the friction applied to the walls of blood vessels, which is difficult to obtain with current measurement techniques. We analyzed hemodynamic data and measured WSS in the area where the LSA was most compressed. In Figure 4(b), WSS in the chimney stent of LSA increased after ch-TEVAR (preoperation vs postoperation: 0.14 Pa vs 23.5 Pa in Case 1 and 0.19 Pa vs 48.3 Pa in Case 2).

It is difficult to measure true blood pressure within the aorta at follow-up, so we used simulated blood pressure measured in the software as a reference. There was no significant difference in blood pressure between aortic arch,

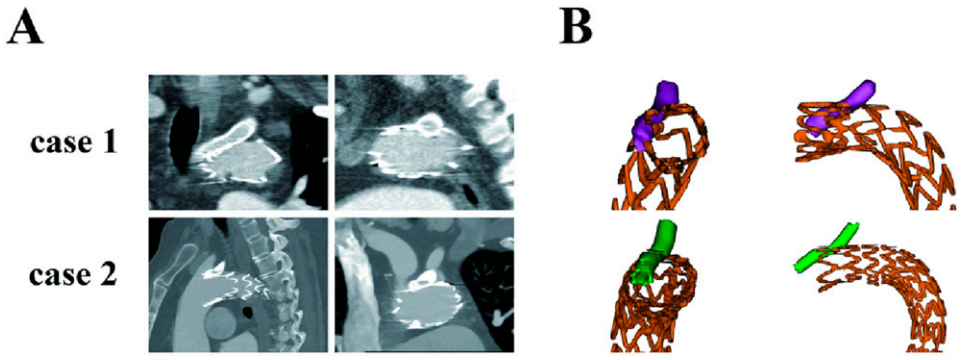

Figure 3. (a) Postoperative CTA of Case 1 and Case 2: The chimney stent was squeezed by the main stent, which was more obvious in Case 2. (b) The position of the support after modeling: Case 2's chimney stent was situated atop the primary chimney, and even twist, and Case 1's chimney stent was placed straight on one side of the main stent.

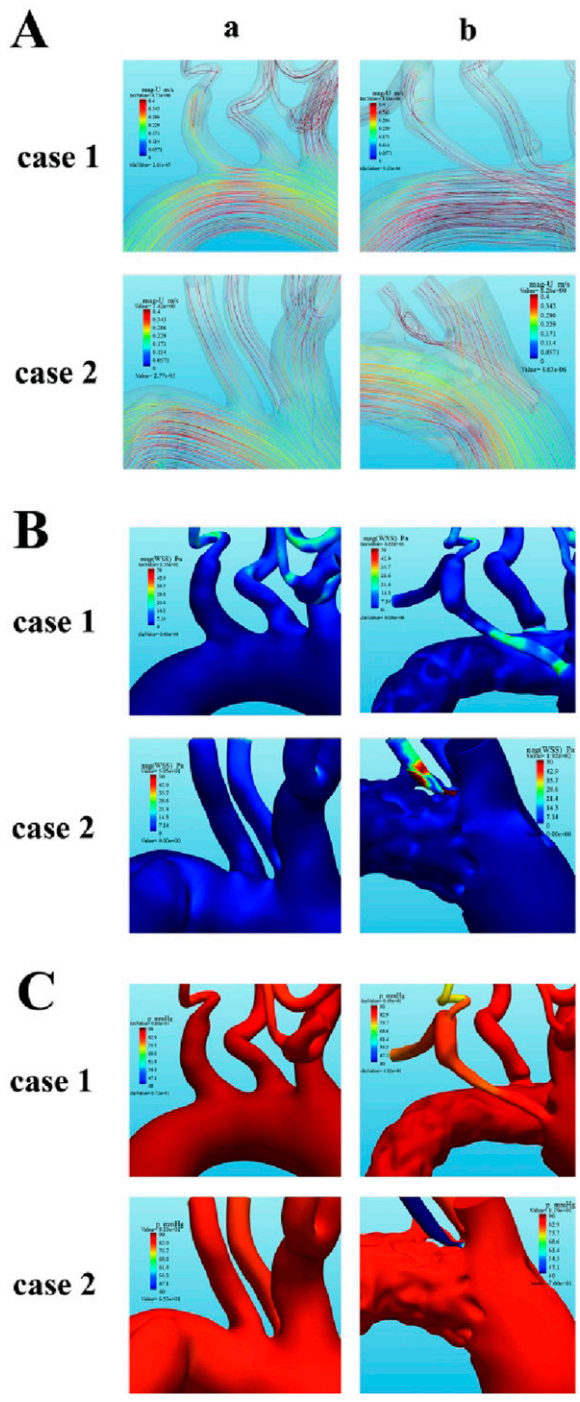

Figure 4. Hemodynamic simulation of blood flow velocity, WSS, and blood pressure of Case 1 and Case 2. (a) The blood velocity of the aorta and its major branches in Case 1 and Case 2 before and after ch-TEVAR. (b) The WSS of the aorta and its major branches in Case 1 and Case 2 before and after ch-TEVAR. (c) The blood pressure of the aorta and its major branches in Case 1 and Case 2 before and after ch-TEVAR.

brachiocephalic trunk, left common carotid artery, and descending aorta after ch-TEVAR, but the blood pressure decreased in LSA after chimney stent; the simulated blood pressure was significantly reduced in Case 2 with LSA near occlusion as show in Figure 4(c). The postoperative blood pressure of Case 2 was 4% of that preoperative. Fortunately, this patient, probably due to vertebral steal, had a normal pulse in his left arm at follow-up, but his blood pressure was markedly lower in the left arm than in the right. The hemodynamic parameter values collected from CFD simulations are show in Tables 1–3.

Discussion

Endoleak has long been thought to contribute to the failure of TEVAR. Gutters, which are unfilled spaces between the main stent and the chimney stent due to incomplete opposition, have been associated with a higher incidence of type I endoleak in ch-TEVAR.[24–26] The radial support forces of the main and chimney stents differ, and their combination affects endoleak occurrence. Kwiecinski et al. used different combinations of chimney stents to analyze the gutter and lumen compression. They concluded that Viabahn, as a chimney stent, presented lower gutter areas and increased lumen compression than other.[27] In our study, when Viabahn chimney stent was compressed, no substantial gutter was observed in any of the patients, and no endoleak occurred. We believe that the main stent and the chimney stent fit each other when squeezed and reduce the gutters, thus reducing the risk of endoleak. We agree with Kwiecinski et al that the Viabahn, as a chimney stent, is a good option to reduce the incidence of endoleak.

The patency of the chimney stent represents a crucial issue within the chimney technique. These stents are not designed to be deployed next to each other, so stent compression or kinking can also affect graft patency.[28,29] Although prior research has indicated that the primary patency rate of the chimney stent could reach 97%–99%.[30] Regrettably, in this study, the stent of Case 2 experienced excessive constriction, resulting in a substantially reduced in-stent blood pressure compared to pre-surgery.

We analyzed the anatomic position and shape of two chimney stents and found that Case 2's chimney stent was situated atop the primary chimney, and even twist, and this stent is most compressed and nearly occluded at the twist part, while Case 1's chimney stent was placed straight on one side of the main stent and was less compressed than in Case 2. The WSS increases correspondingly where chimney stent is obviously compressed. In Case 2, the increase of WSS was most obvious where the chimney stent was most compressed, and a lot of turbulence occurred. Previous

Table 1. Blood pressure of the aorta and its major branches in the three patients before and after ch-TEVAR.

	Case 1		Case 2	
Blood pressure (mmHg)	Before TEVAR	After TEVAR	Before TEVAR	After TEVAR
Aortic arch	86.86	86.70	81.67	81.52
Brachiocephalic trunk	86.23	85.93	81.47	81.19
Left common carotid artery	86.02	83.64	80.62	81.35
Left subclavian artery	86.66	79.03	81.24	4.06
Aorta descendens	80.02	84.71	80.62	85.43

Table 2. WSS of the aorta and its major branches in the three patients before and after ch-TEVAR.

	Case 1		Case 2	
WSS (Pa)	Before TEVAR	After TEVAR	Before TEVAR	After TEVAR
Aortic arch	0.03	0.02	0.02	0.02
Brachiocephalic trunk	0.39	0.27	0.09	0.08
Left common carotid artery	0.58	0.63	0.40	0.45
Left subclavian artery	0.14	23.5	0.19	48.3
Aorta descendens	0.04	0.22	0.08	0.08

Table 3. Blood velocity of the aorta and its major branches in the three patients before and after ch-TEVAR.

	Patient 1		Patient 2	
Blood velocity (m/s)	Before TEVAR	After TEVAR	Before TEVAR	After TEVAR
Aortic arch	0.21	0.21	0.20	0.19
Brachiocephalic trunk	0.40	0.39	0.23	0.23
Left common carotid artery	0.39	0.47	0.41	0.46
Left subclavian artery	0.18	0.60	0.25	0.70
Aorta descendens	0.26	0.35	0.25s	0.29

research has demonstrated that heightened WSS and the resulting intricate turbulence in severely compressed stents may instigate the activation of local high-shear thrombus pathways, leading to LSA chimney stent occlusion.[31,32] Therefore, we believe that the position and shape of chimney stent affect its patency rate. The chimney stent should be straight on one side of the main stent and avoid twist, so as to avoid the block of LSA and ensure the efficacy of ch-TEVAR.

In this study, all patients utilized the Viabahn, a covered stent as the chimney stent and exhibited various degrees of aortic insertion. Some hemodynamic analyses of fenestrated covered stents revealed insertion into the aorta, with turbulence and thrombosis frequently occurring around the inserted segment of this stent.[33,34] Concerns were raised regarding the potential impact of the inserted segment of the chimney stent on hemodynamic of the aortic arch and its major branches. Upon constructing the hemodynamic model, we found that alterations in the aortic arch and its major branches like carotid artery and trunk brachiocephalic artery were minimal.

As a limitation of this study, the hemodynamic analysis of chimney stent in ch-TEVAR remains to be studied with a large sample of clinical data. Furthermore, this study regarded aortic and stents as rigid walls, but the aortic and the stents have deformation under the blood flow which may affect the accuracy of prediction. In the future, more reasonable patient-specific model will be constructed and the fluid–structure interaction method will be applied to study hemodynamics after TEVAR.

Conclusions

Our patient-specific simulation outcomes confirm previous research that the chimney stent can fit to the main stent, reducing the gutter and the endoleak. However, it is crucial to note that stents should be positioned on both sides of the main stent and maintained in a straight alignment to avoid

occlusion. Otherwise, it may produce severe hemodynamic changes in LSA. In addition, the chimney stent had little effect on the hemodynamics of the other branches of the aorta arch and the visceral segment of the descending aorta.

Declaration of Conflicting Interests

The author(s) declared no potential conflicts of interest with respect to the research, authorship, and/or publication of this article.

Funding

The author(s) disclosed receipt of the following financial support for the research, authorship, and/or publication of this article: This work was supported by Medical Scientific Research Foundation of Zhejiang Province (grant numbers 2021ky293 and 2021ky299) and Project of NINGBO Leading Medical &Health Discipline (grant numbers 2022-F21).

Ethical statement

This work was approved by the Ethics Committee of Ningbo No.2 hospital (approval number: YJ-KYSB-NBEY-2020-084-01). Written informed consent has been obtained from the patients for publication of the case report and accompanying images.

ORCID iD

Yunpeng Ding https://orcid.org/0000-0003-4509-0233

References

1. Dake MD, Miller DC, Semba CP, et al. Transluminal placement of endovascular stent-grafts for the treatment of descending thoracic aortic aneurysms. *N Engl J Med* 1994; 331: 1729-1734. DOI: 10.1056/nejm199412293312601.
2. Alfson DB and Ham SW. Type B aortic dissections: current guidelines for treatment. *Cardiol Clin* 2017; 35: 387-410. DOI: 10.1016/j.ccl.2017.03.007.
3. Yoon WJ and Mell MW. Outcome comparison of thoracic endovascular aortic repair performed outside versus inside proximal landing zone length recommendation. *J Vasc Surg* 2020; 72: 1883-1890. DOI: 10.1016/j.jvs.2020.03.033.
4. Mesar T, Alie-Cusson FS, Rathore A, et al. A more proximal landing zone is preferred for thoracic endovascular repair of acute type B aortic dissections. *J Vasc Surg* 2022; 75: 38-46. DOI: 10.1016/j.jvs.2021.06.036.
5. Riambau V, Böckler D, Brunkwall J, et al. Editor's choice - management of descending thoracic aorta diseases: clinical practice guidelines of the European society for vascular surgery (ESVS), editor's choice - management of descending thoracic aorta diseases: clinical practice guidelines of the European Society for Vascular Surgery (ESVS). *Eur J Vasc Endovasc Surg* 2017; 53: 4-52. DOI: 10.1016/j.ejvs.2016.06.005.
6. Czerny M, Schmidli J, Adler S, et al. Editor's choice - current options and recommendations for the treatment of thoracic aortic pathologies involving the aortic arch: an expert consensus document of the European association for cardio-thoracic surgery (EACTS) & the European society for vascular surgery (ESVS). *Eur J Vasc Endovasc Surg* 2019; 57: 165-198. DOI: 10.1016/j.ejvs.2018.09.016.
7. Matsumura JS, Lee WA, Mitchell RS, et al. The Society for Vascular Surgery Practice Guidelines: management of the left subclavian artery with thoracic endovascular aortic repair. *J Vasc Surg* 2009; 50: 1155-1158. DOI: 10.1016/j.jvs.2009.08.090.
8. Tanaka A and Estrera A. Endovascular treatment options for the aortic arch. *Cardiol Clin* 2017; 35: 357-366. DOI: 10.1016/j.ccl.2017.03.005.
9. Anwar MA and Hamady M. Various endoluminal approaches available for treating pathologies of the aortic arch. *Cardiovasc Intervent Radiol* 2020; 43: 1756-1769. DOI: 10.1007/s00270-020-02561-y.
10. Shu C, Fan B, Luo M, et al. Endovascular treatment for aortic arch pathologies: chimney, on-the-table fenestration, and in-situ fenestration techniques. *J Thorac Dis* 2020; 12: 1437-1448. DOI: 10.21037/jtd.2020.03.10.
11. Criado FJ, Barnatan MF, Rizk Y, et al. Technical strategies to expand stent-graft applicability in the aortic arch and proximal descending thoracic aorta. *J Endovasc Ther* 2002; 9(-Suppl 2): Ii32-38.
12. Li J, Xue Y, Li S, et al. Outcomes of thoracic endovascular aortic repair with chimney technique for aortic arch diseases. *Front Cardiovasc Med* 2022; 9: 868457. DOI: 10.3389/fcvm.2022.868457.
13. Wu M, Zhao Y, Zeng Z, et al. Mid-term comparison of one-piece branched stent-graft and chimney technique treating aortic arch pathologies. *Cardiovasc Intervent Radiol* 2022; 45: 733-743. DOI: 10.1007/s00270-022-03063-9.
14. Zou J, Jiao Y, Zhang X, et al. Early- and mid-term results of the chimney technique in the repair of aortic arch pathologies. *Cardiovasc Intervent Radiol* 2016; 39: 1550-1556. DOI: 10.1007/s00270-016-1439-6.
15. Ahmad W, Mylonas S, Majd P, et al. A current systematic evaluation and meta-analysis of chimney graft technology in aortic arch diseases. *J Vasc Surg* 2017; 66: 1602–1610. DOI: 10.1016/j.jvs.2017.06.100.
16. Pecoraro F, Veith FJ, Puippe G, et al. Mid- and longer-term follow up of chimney and/or periscope grafts and risk factors for failure. *Eur J Vasc Endovasc Surg* 2016; 51: 664-673. DOI: 10.1016/j.ejvs.2016.01.010.
17. Sun Z and Chaichana T. A systematic review of computational fluid dynamics in type B aortic dissection. *Int J Cardiol* 2016; 210: 28-31. DOI: 10.1016/j.ijcard.2016.02.099.
18. Malkawi AH, Hinchliffe RJ, Xu Y, et al. Patient-specific biomechanical profiling in abdominal aortic aneurysm development and rupture. *J Vasc Surg* 2010; 52: 480-488. DOI: 10.1016/j.jvs.2010.01.029.
19. Numata S, Itatani K, Kanda K, et al. Blood flow analysis of the aortic arch using computational fluid dynamics.

Eur J Cardio Thorac Surg 2016; 49: 1578-1585. DOI: 10.1093/ejcts/ezv459.

20. Kim HJ, Vignon-Clementel IE, Figueroa CA, et al. On coupling a lumped parameter heart model and a three-dimensional finite element aorta model. *Ann Biomed Eng* 2009; 37: 2153-2169. DOI: 10.1007/s10439-009-9760-8.
21. Westerhof N, Bosman F, De Vries CJ, et al. Analog studies of the human systemic arterial tree. *J Biomech* 1969; 2: 121-143. DOI: 10.1016/0021-9290(69)90024-4.
22. Li Z and Mao W, A fast approach to estimating windkessel model parameters for patient-specific multi-scale cfd simulations of aortic flow, *Computers & Fluids* 2023; 259: 105894. DOI: 10.1016/j.compfluid.2023.105894.
23. Alastruey J, Xiao N, Fok H, et al. On the impact of modelling assumptions in multi-scale, subject-specific models of aortic haemodynamics. *J R Soc Interface* 2016; 13: 17. DOI: 10.1098/rsif.2016.0073.
24. Li C, de Guerre L, Dansey K, et al. The impact of completion and follow-up endoleaks on survival, reintervention, and rupture. *J Vasc Surg* 2023; 77: 1676-1684. DOI: 10.1016/j.jvs.2023.02.009.
25. Moulakakis KG, Mylonas SN, Dalainas I, et al. The chimney-graft technique for preserving supra-aortic branches: a review. *Ann Cardiothorac Surg* 2013; 2: 339-346. DOI: 10.3978/j.issn.2225-319X.2013.05.14.
26. Li Y, Zhang T, Guo W, et al. Endovascular chimney technique for juxtarenal abdominal aortic aneurysm: a systematic review using pooled analysis and meta-analysis. *Ann Vasc Surg* 2015; 29: 1141-1150. DOI: 10.1016/j.avsg.2015.02.015.
27. Kwiecinski J, Cheng CP, Uberoi R, et al. Thoracic aortic parallel stent-graft behaviour when subjected to radial loading. *J Mech Behav Biomed Mater* 2021; 118: 104407. DOI: 10.1016/j.jmbbm.2021.104407.
28. Baldwin ZK, Chuter TA, Hiramoto JS, et al. Double-barrel technique for preservation of aortic arch branches during thoracic endovascular aortic repair. *Ann Vasc Surg* 2008; 22: 703-709. DOI: 10.1016/j.avsg.2008.06.002.
29. Atkins MD and Lumsden AB. Parallel grafts and physician modified endografts for endovascular repair of the aortic arch. *Ann Cardiothorac Surg* 2022; 11: 16-25. DOI: 10.21037/acs-2021-taes-171.
30. Lindblad B, Bin Jabr A, Holst J, et al. Chimney grafts in aortic stent grafting: hazardous or useful technique? Systematic review of current data. *Eur J Vasc Endovasc Surg* 2015; 50: 722-731. DOI: 10.1016/j.ejvs.2015.07.038.
31. Raptis A, Xenos M, Spanos K, et al. Endograft specific haemodynamics after endovascular aneurysm repair: flow characteristics of four stent graft systems. *Eur J Vasc Endovasc Surg* 2019; 58: 538-547. DOI: 10.1016/j.ejvs.2019.04.017.
32. Midulla M, Moreno R, Negre-Salvayre A, et al. Impact of thoracic endografting on the hemodynamics of the native aorta: pre- and postoperative assessments of wall shear stress and vorticity using computational fluid dynamics. *J Endovasc Ther* 2021; 28: 1526602820959662-1526602820959669. DOI: 10.1177/1526602820959662.
33. Sengupta S, Hamady M and Xu XY. Haemodynamic analysis of branched endografts for complex aortic arch repair. *Bioengineering (Basel, Switzerland)* 2022; 9: 45. DOI: 10.3390/bioengineering9020045.
34. Tricarico R, Tran-Son-Tay R, Laquian L, et al. Haemodynamics of different configurations of a left subclavian artery stent graft for thoracic endovascular aortic repair. *Eur J Vasc Endovasc Surg* 2020; 59: 7-15. DOI: 10.1016/j.ejvs.2019.06.028.